Verification of the ozone algorithmic climate change functions for predicting the short-term NOx effects from aviation en-route

Yin, Feijia; Grewe, Volker; van Manen, Jesper; Matthes, Sigrun ; Yamashita, Hiroshi; Linke, Florian; Lührs, Benjamin

Publication date
2018

Document Version
Final published version

Published in
ICRAT 2018: 2018 International Conference on Research in Air Transportation

Verification of the ozone algorithmic climate change functions for predicting the short-term NO_x effects from aviation en-route

Feijia Yin*, Volker Grewe†, Jesper van Manen
Faculty of Aerospace Engineering
Delft University of Technology
Delft, the Netherlands
*corresponding author: F.yin@tudelft.nl
† also at Institut für Physik der Atmosphäre
Deutsches Zentrum für Luft- und Raumfahrt
Wessling, Germany

Sigrun Matthes, Hiroshi Yamashita
Institut für Physik der Atmosphäre
Deutsches Zentrum für Luft- und Raumfahrt
Wessling, Germany

Florian Linke, Benjamin Lührs
Institut für Lufttransportsysteme
Deutsches Zentrum für Luft- und Raumfahrt
Hamburg, Germany

***Abstract*—For the first time, the algorithmic Climate Change Functions (aCCFs) for ozone, methane, water vapor, and persistent contrails have been developed within the ATM4E project to provide information on the climate sensitive regions, which can be conveniently implemented for the climate based flight routing. These aCCFs need to be verified before they are implemented. In this paper, we focus on the verification of the ozone aCCFs to enable the prediction of the short-term NO_x effects from aviation en-route. The verification is conducted from two aspects. Firstly, the climatology of the ozone aCCFs is calculated based on a one-year simulation and verified by the existing literature. Secondly, the effectiveness of the ozone aCCFs for optimizing aircraft trajectories concerning the climate impact is verified by the comprehensive climate-chemistry model calculation.**

Keywords-Verification; aCCFs; flight routing; minimal climate impact;

I. INTRODUCTION

Civil aviation, on the one hand, is the driver of global growth, is increasing at around 4.7% per annum, and is poised to maintain that growth for next few decades [1], but on the other hand, the environmental impact of aviation is increasing at a rapid pace. Advancements in technology and operations have managed to reduce fuel consumption (and thereby the CO_2 emission) per passenger km by around 70% in the last 5-6 decades. Even though currently aviation emits only 2.5% of the global CO_2, it is responsible for 5% of global warming [2, 3]. This is because the non-CO_2 emissions from aircraft in the uppermost troposphere or the lowermost stratosphere are as harmful to global warming as CO_2.

The non-CO_2 effects, from methane depletion and ozone formation due to NO_x [4], the contrails formed by water vapor combined with aerosols, and the water vapor itself, depend on not only the quantity of emissions, but also the altitude, geographical location, time and the local weather conditions acting on different spatial and temporal scales. This provides the opportunities to mitigate the aviation's climate impact beyond CO_2 via the operational measures to avoid the climate sensitive regions associated to the non-CO_2 effects. To enable the climate-based operations, the information on the climate sensitive regions needs to be available. In the ATM4E (Air Traffic Management for Environment) project, the so-called algorithmic Climate Change Functions (aCCFs) have been developed to serve this purpose [5, 6].

Here, we present results of the ATM4E project, focusing on the verification of the ozone aCCFs, from two aspects: (1) verify the ozone aCCFs climatology and (2) verify the effectiveness of the ozone aCCFs to reduce the climate impact caused by NO_x-ozone effects.

II. THE ALGORITHMIC CLIMATE CHANGE FUNCTIONS

Climate Change Functions (CCFs, [7, 8]) are 5D datasets (longitude, latitude, altitude, time, type of emission), which describe the specific climate impacts, i.e. the anticipated climate change for a local emission, or in other words, the climate change per flown kilometer and per emitted masses of the relevant species. Within the EU-project REACT4C (www.react4c.eu) high fidelity CCFs were computed for eight representative weather situations for the North Atlantic [9, 10].

To establish relations between localized emissions and their impact on climate, the ECHAM/MESSy Atmospheric Chemistry (EMAC) model was applied. The emissions were released at roughly 500 points in the atmosphere in the North-Atlantic region. The transport of these emitted species is calculated by 50 air parcel trajectories, and microphysical processes are included to simulate contrail formation, ice particle sedimentation, and sublimation. A detailed chemical mechanism provides the evolution of contributions of the initial NO_x emission to the greenhouse gases ozone and methane. Washout processes (rain) and dry deposition are parameterized to account for the removal of the emitted species. Radiation calculation provides radiative forcing (RF; stratosphere adjusted) of the changes due to contrails and ozone, and radiation parameterizations provide estimates for the RF from water vapor, ozone, methane, and carbon dioxide. These are then fed into climate metrics to provide estimates of the climate impact. Here we concentrate on one of the metrics, the average temperature response over 20 years (ATR20) since the results are almost independent of the chosen metric [11]. The CCFs were calculated for five representative winter and three summer weather situations, following classification of Irvine [12]. Fig. 1 shows exemplarily the winter weather pattern 2 (WP2) with a strong jet (dark blue) and a high-pressure ridge, which reaches from Africa to the tip of Greenland. In this high-pressure ridge, the ozone CCF shows a maximum.

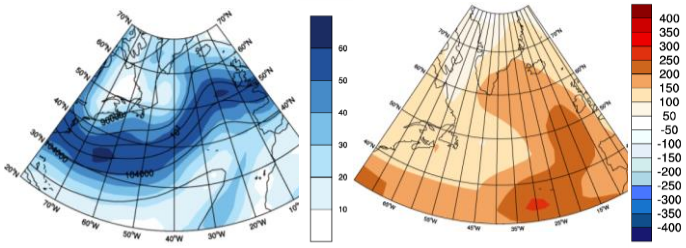

Fig. 1: Ozone climate change function for weather pattern 2: Left: geopotential (isolines, m^2/s^2) and wind speed (color, m/s); Right: ozone CCF (10^{-14} K/kg(NO_2)) [9]. Note that the left figure has a slightly larger cut-out.

The calculation of these CCFs requires a large amount of computing time. It is not applicable to numerical weather forecasts. Therefore, within ATM4E, we have started to develop algorithmic climate change functions (aCCFs), which represent a correlation of the weather system at the time of emission and the respective CCFs, which can easily be implemented in any numerical weather prediction model (NWP) and thereby advancing the MET-Services.

We have developed these functions for all regarded effects, i.e. the impact of water vapor emissions on climate, NO_x emissions on ozone and methane separately [6], and the impact on contrails, separated for day and night contrails. Here we present exemplarily the O_3 aCCFs, where

$$ATR20_{O_3} = \beta_0 + \beta_1 \cdot T + \beta_2 \cdot geopot + \beta_3 \cdot T \cdot geopot \quad (1)$$

With β_0=-5.2e-11 K/kg-NO_2, β_1=2.3e-13 K/K/kg-NO_2, β_2=4.85e-16 K/kg-NO_2/(m^2s^{-2}), β_3=-2.04e-18 K/K/kg-NO_2/(m^2s^{-2}), T is the temperature in K, and geopot is the geopotential in m^2s^{-2}. Fig. 2 shows an example of the temperature response calculated from the ozone aCCFs on a specific day over the European region at 200 hPa. In the following sections, we will verify the effectiveness of this ozone aCCFs.

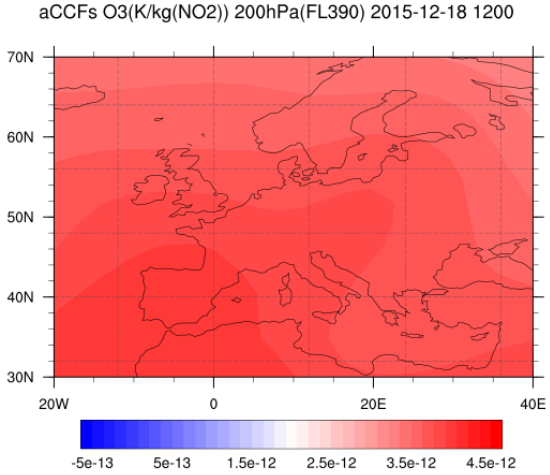

Fig. 2: The temperature response (K/kg(NO_2)) calculated by the ozone aCCFs on a specific day 1200 hour at 200 hPa.

III. THE VERIFICATION APPROACH

The verification of the ozone aCCFs is performed from two aspects:

- To verify the climatology of the ozone aCCFs
- To verify the effectiveness of the ozone aCCFs to reduce the climate impact caused by NO_x-O_3 from a subset of European flights on the daily basis

The present air traffic simulation is performed using the EMAC model. The EMAC model is a numerical chemistry and climate simulation system that includes sub-models describing tropospheric and middle atmosphere processes and their interaction with oceans, land and human influences [13]. It uses the second version of the Modular Earth Sub-model System (MESSy2) [14, 15] to link multi-institutional computer codes. The core atmospheric model is the 5th generation European Centre Hamburg general circulation model (ECHAM5) [16, 17]. For the present study, the sub models: AirTraf [18], TAGGING [19], RAD [20], and aCCFs are used.

A. The flight trajectory optimization tool (AirTraf)

Identify applicable sponsor/s here. *(sponsors)*

To analyze the impact on the atmospheric changes (exemplarily O_3 in the current analysis) caused by changing the flight routes, the first step has been to calculate the flight trajectories. The flight trajectories are calculated using EMAC/AirTraf [13, 21]. AirTraf is a 4D trajectory simulation tool running on the EMAC platform [18]. It optimizes flight trajectories at cruise level with respect to different objectives, e.g., great circle or minimal flight time, considering the local weather conditions. The unique feature of AirTraf combined with EMAC provides the opportunity to assess the impact of aviation emissions, resulting from aircraft trajectory optimization on the atmospheric composition and RF.

An overview of the AirTraf principle can be found in Fig. 3. Before the simulation starts, the initial data are required, including city pairs, flight timetables, and the performance characteristics of the aircraft/engine. Depending on the aircraft routing options, the flight trajectory is calculated until the aircraft reaches its destination. The resulting fuel consumption and emissions are calculated and gathered afterward. The output files contain the coordinates of the aircraft (latitude, longitude, and altitude), flight time, flight distance, fuel consumption, and emissions (NO_x and H_2O). The fuel flow rates and emissions are calculated using the total energy model based on the Eurocontrol's Base of Aircraft Data (BADA) method [22] and the DLR fuel flow method [23] for a specific aircraft type used. The engine performance data is taken from the International Civil Aviation Organization (ICAO) database [24].

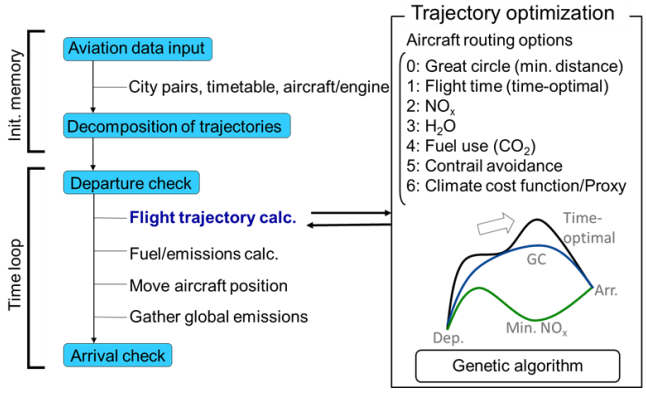

Fig. 3: An overview of the AirTraf simulation tool [21].

In the climate optimal routing option, the algorithm-based Climate Change Functions (aCCFs) developed within the ATM4E project are implemented [6]. The aCCFs provide the average temperature response in 20 years (ATR20) for different non-CO_2 effects, e.g., ozone, methane, water vapour and contrails, attributed to the changes of their quantities and the emitted locations. The ATR20s are then fed to the trajectory optimization routing to minimize the climate impact of aircraft.

B. The sub model TAGGING: Tracking contributions from emissions to atmospheric concentrations

The sub model TAGGING, described by Grewe et al. [19], is a diagnostic, which allows quantifying the impact of emission sources on the atmospheric composition. It is an accounting system following the reaction pathways from emissions of specific sources. Ten different chemical species and families are tagged: ozone, carbon monoxide, PAN, NO_y, NMHCs, OH, and HO_2. Ten different source categories are distinguished, which include natural emissions (e.g., lightning, soils) and anthropogenic emissions (e.g., industry, road traffic, shipping, aviation). In the current verification, we tag two aviation source categories: background air traffic and the air traffic optimized by AirTraf. We are concentrating on the emissions from optimized aircraft trajectories based on the sub-model AirTraf, only, and diagnose atmospheric changes with the TAGGING sub model.

C. The sub model RAD: Calculation of the Radiative Forcing

The sub model RAD [20] calculates the amount of long- and short- wave radiation traveling through the atmosphere. It takes into account radiation changes induced by clouds, aerosols, albedo, and greenhouse gases (both natural and anthropogenic emissions). Here we are analyzing the difference in radiation from all the effects aforementioned minus the radiation when the ozone produced by the emissions from the optimized air traffic is subtracted. This difference eventually defines the radiative forcing of the ozone effect from the optimized air traffic.

IV. RESULTS

A. The verification of the ozone aCCFs climatology

To verify the climatology of the ozone aCCFs, we calculate the zonal mean of the ozone aCCFs based on one-year simulation. The zonal mean value is then multiplied by the emission scenario as given in Table 1 [25]. The resulted mean surface temperature changes from ozone aCCFs (Fig. 4) are compared with the results in [25]. The variation pattern of the ozone aCCFs matches well with the literature results over the northern hemisphere (the latitude between 30° N and 90°N) and the flight corridor (roughly 9km to 12 km vertical range)

Table 1: Description of the applied aircraft emission dataset

Project	Abbr.	Year	Descriptions	Fuel [Tg/a]	EI(NO_x) [g/kg (fuel)]
SCENIC	S4	2050	Subsonic air traffic	677	10.85

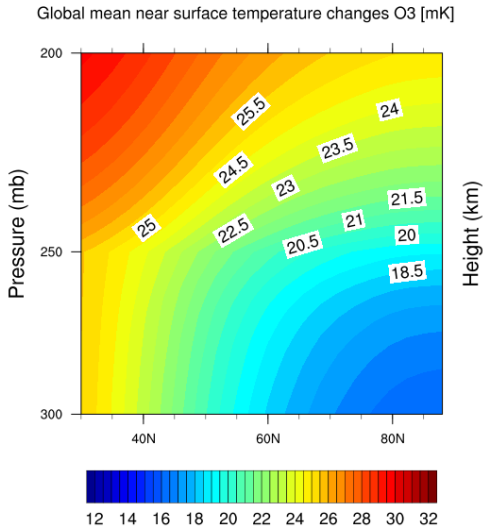

Fig. 4: Mean near surface temperature changes (mK) in the confined field attributed to O_3 concentration change caused by NO_x emissions.

B. The effectiveness of the climate optimization with daily routes analysis

Two simulations with daily air traffic are performed. In the first simulation, the air traffic trajectories are optimized concerning costs and in the second concerning climate impact, which is described by the aCCFs. In both simulations, the NO_x emissions alter differently ozone and the Radiative Forcing (RF). The reduction of the RF in the situation of climate-optimized routes proofs the concept of algorithmic climate changes functions (see Fig. 5).

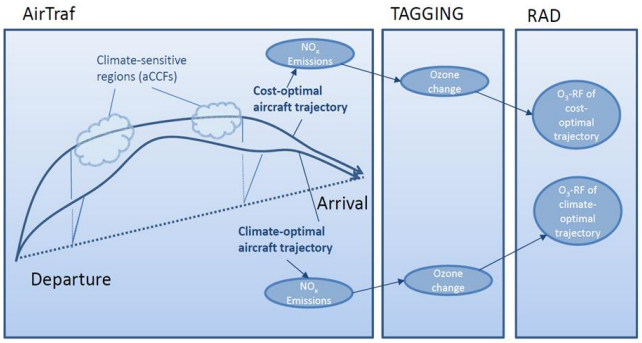

Fig. 5: Sketch of the performed simulations and used EMAC sub models (boxes).

The simulation setup is given in Table 2. A subset of one day European flights selected in the ATM4E is used. The constant flight Mach number 0.82 combined with the wind speed will result in the different ground speeds. For the cost optimal flights, the operating cost, calculated using Eqn. (1), is the objective function, whereas, for the climate optimal flights, the O_3-ATR20 is used as the objective function. There are 11 design variables, among which, five variables control the vertical change between [FL290, FL410] and six variables control the lateral change. The Adaptive Range Multi-objective Genetic Algorithm (ARMOGA version 1.2.0, [26, 27]) is implemented for the trajectory optimization. The EMAC model resolution is 2.8 by 2.8 degrees in latitude and longitude and 31 vertical levels up to an altitude of roughly 30 km (10 hPa)

$$\cos t = C_t \cdot t + C_f \cdot m_{fuel} \quad (1)$$

Where t is the flight time in hrs, m_{fuel} is the fuel consumption in kg, C_t is the flight time-related cost in €/hr; C_f is the fuel-related cost in €/kg(fuel).

Table 2: Trajectory optimization setup

AirTraf Options	Cost optimal	Climate optimal
EMAC Resolution	T42/L31ECMWF (2.8° × 2.8° in latitude and longitude, 31 vertical pressure levels up to 10 hPa)	
Waypoints	101	
Flight plan	85 European flights	
Aircraft/Engine type	One given aircraft/engine model	
EI H_2O [g/kg(fuel)]	1230 (IPCC 1999)	
Load factor	0.62 (ICAO 2009)	
Mach number	0.82	
Flight altitude	[FL290, FL410]	
Optimization objective	Cost	O_3-ATR20
Design variable	11 (Location 6/Altitude 5)	
Optimization approach	Genetic algorithm	

In Fig. 6 and Fig. 7, the flight trajectories for the minimal cost (Fig. 6) and the minimal climate impact (Fig. 7) are presented. The cost depends on the flight time and the fuel consumption. Though, there might be favorable wind conditions at the lower altitude, which is beneficial to shorten the flight time, the optimization routine still chooses the flights with the highest altitude within the vertical constraints. The season is because flying at higher altitude reduces the fuel consumption, which dominates the overall operating cost in most cases.

As for the climate optimal flights, the situation is more complicated, since the temperature response of ozone attributed to the NO_x emissions depends on multi-criterions, e.g., the emitted quantity, time, location and the weather condition. On average, the altitudes of the climate optimal flights are lower than the cost-optimal flights. Lateral changes have also been observed in several trajectories contributing to the reduction of the climate impact of NO_x emissions.

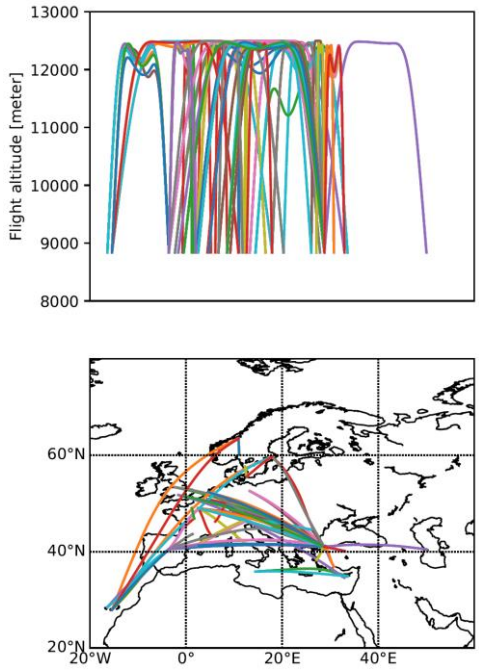

Fig. 6: Daily flight trajectories calculated using AirTraf for the cost optimal

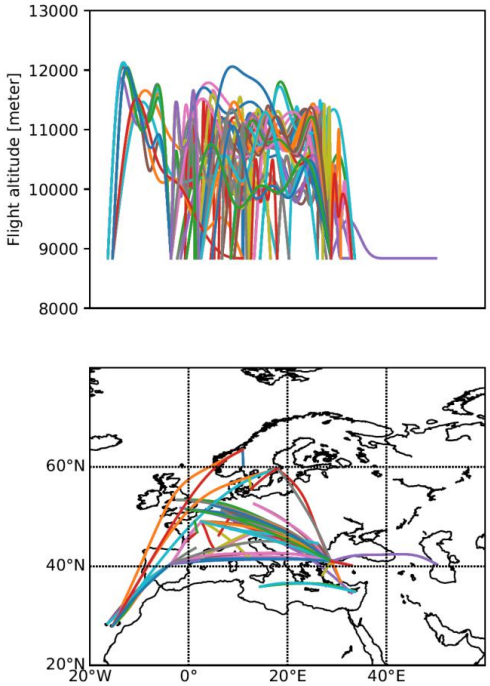

Fig. 7: Daily flight trajectories calculated using AirTraf for the climate optimal only considering the NO_x-O_3 effects.

The flight characteristics are presented in Table 3. Compared to the cost optimal flights, the fuel consumption of the climate optimal flights is 11% more and the NO_x emissions are 15% more. The total cost of the climate optimal flights is 5% higher than the cost optimal flights.

Table 3: Monthly mean characteristics of the cost optimal flights and the climate optimal flight

Parameters	Cost optimal	Climate optimal
Fuel consumption [Tons]	728	810
NO_x emissions [Tons]	7.26	8.33
Flight time [hrs]	157	156
Flight distance [km]	134000	134346
Cost [k€]	636.56	667.76

C. Ozone concentration changes

Fig. 8 and Fig. 9 present the mean NO_x emission for the cost optimal flights (Fig. 8) and the climate optimal flights (Fig. 9), respectively. We can see the climate optimal flights emit NO_x at a lower altitude between 300 hPa (=mb) and 200 hPa, whereas, the cost optimal flights emit NO_x at vertical level-up to 100 hPa, directly in the stratosphere.

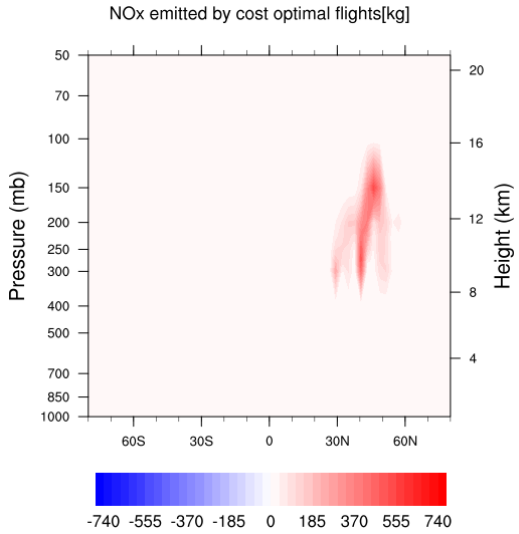

Fig. 8: Monthly zonal mean NO_x in kg emitted by the cost optimal flights.

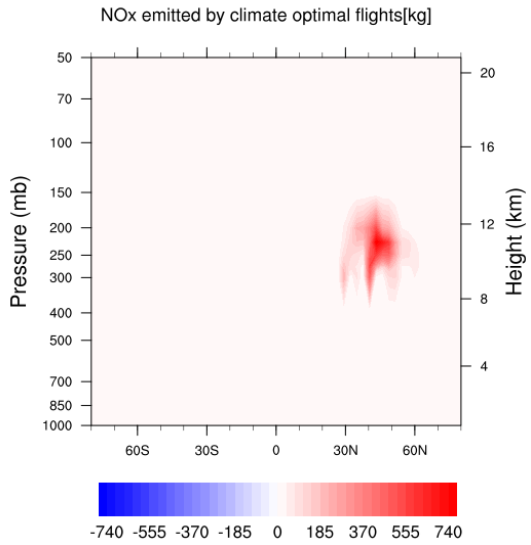

Fig. 9: Monthly zonal mean NO_x in kg emitted by the climate optimal flights.

Fig. 10 presents the difference in the NO_x between the climate optimal routes and the cost optimal routes. Since most of the NO_x is emitted at lower altitudes in the climate optimal routing case, also NO_x concentration is lower at higher altitudes and higher at lower altitudes for the climate optimal flights compared to the cost optimal flights. The residence time of NO_x is shorter at the lower altitudes due to more active chemistry and enhanced rain out, therefore, the reduction in NO_x at the higher altitude is more pronounced than the increase at lower altitudes.

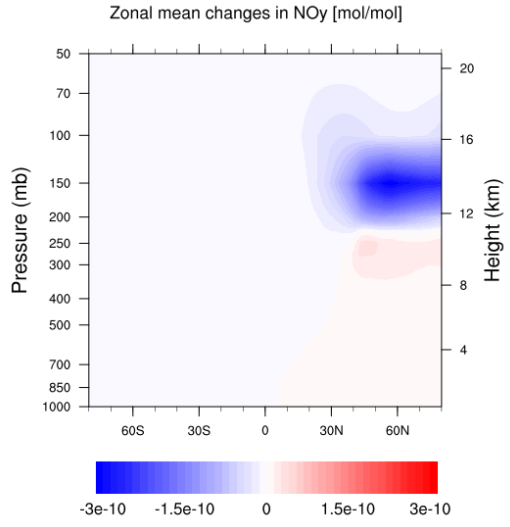

Fig. 10: The changes of the atmospheric NO_x-concentration (mol/mol) caused by climate optimal flights compared to the cost optimal flights.

The changes in the NO_x location cause an increase in ozone at lower altitudes and the reduction in ozone at higher altitudes as can be seen from Fig. 11. By comparing our calculation results with the REACT4C studies in [28], we can see the variation pattern on the changes in O_3 by lowering the flight altitude matches well.

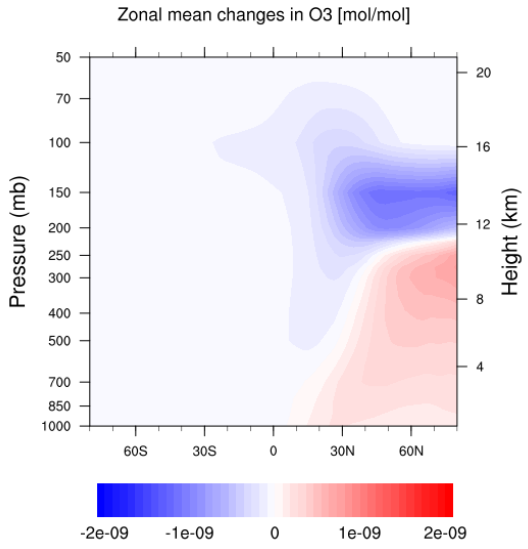

Fig. 11: Ozone changes (mol/mol) arising from flying climate optimal routes compared to cost optimal flights

D. Radiative forcing calculation

The O_3 radiative forcing (RF) has been calculated for the cost optimal flights and the climate optimal flights. The mean RF for O_3 is presented in Table 4. Compared to the cost optimal flights, the climate optimal flights have smaller LW forcing and larger the SW forcing, which results in the negative O_3 radiative forcing of about -0.3 mW/m^2. This is largely because of the reduction in flight altitude.

Table 4: Mean adjusted ozone radiative forcing (mW/m^2) for the cost optimal flight and the climate optimal flights.

	Cost optimal	Climate optimal	Climate_opt-Cost_opt
O_3 RF [mW/m^2]	13.6	13.3	-0.3

V. CONCLUSIONS

In this study, we verify the ozone aCCFs, which were developed in ATM4E, in providing information of the climate sensitive regions for climate-optimized routing. From the analysis, the following conclusions are drawn:

- The variation pattern of the ozone aCCFs matches well with the literature within the northern hemisphere flight corridor: i.e., the vertical range of about 9km to 12 km and the latitude between 30°N and 90°N.

- Altering the flight routes causes the changes in the location of the NO_x emissions. The climate optimal flights emit the NO_x at a lower altitude as compared to the cost optimal flights. Hence, the O_3 in the lower stratosphere decreases, whereas, the O_3 at the lower levels increases for the climate optimal flights. This pattern of the chemical O_3 perturbation and the sensitivity to the altitude of aircraft NO_x emissions is consistent with the REACT4C studies in [28].
- By flying at the lower altitude to avoid the climate sensitive regions, the O_3 net radiative forcing of the climate optimal flights is about 0.3 mW/m^2 less when compared to the O_3 RF of the cost optimal flights, which confirms the effectiveness of the ozone aCCFs for optimizing the flight trajectories to reduce the climate impact.

ACKNOWLEDGMENT

The current study has been supported by the ATM4E project. This project has received funding from the SESAR Joint Undertaking under grant agreement No 699395 under European Union's Horizon 2020 research and innovation program.

REFERENCES

1. *Growing Horizons 2017/2036*, in *Global Market Forecast*, Airbus, Editor. 2017: Airbus: Toulouse, France.
2. Lee, D.S., D.W. Fahey, P.M. Forster, P.J. Newton, R.C.N. Wit, L.L. Lim, B. Owen, and R. Sausen, *Aviation and global climate change in the 21st century.* Atmospheric Environment, 2009. 43(22–23): p. 3520-3537.
3. Lee, D.S., G. Pitari, V. Grewe, K. Gierens, J.E. Penner, A. Petzold, M.J. Prather, U. Schumann, A. Bais, T. Berntsen, D. Iachetti, L.L. Lim, and R. Sausen, *Transport impacts on atmosphere and climate: Aviation.* Atmospheric Environment, 2010. 44(37): p. 4678-4734.
4. Stevenson, D.S., R.M. Doherty, M.G. Sanderson, W.J. Collins, C.E. Johnson, and R.G. Derwent, *Radiative forcing from aircraft NOx emissions: Mechanisms and seasonal dependence.* Journal of Geophysical Research: Atmospheres, 2004. 109(D17): p. n/a-n/a.
5. Matthes, S., V. Grewe, K. Dahlmann, C. Frömming, E. Irvine, L. Lim, F. Linke, B. Lührs, B. Owen, K. Shine, S. Stromatas, H. Yamashita, and F. Yin, *A Concept for Multi-Criteria Environmental Assessment of Aircraft Trajectories.* Aerospace, 2017. 4(3): p. 42.
6. van Manen, J. and V. Grewe, *Algorithmic climate change functions for the use in eco-efficient flight planning.* submitted to Transp. Res. Part D, 2017.
7. Grewe, V., C. Frömming, S. Matthes, S. Brinkop, M. Ponater, S. Dietmüller, P. Jöckel, H. Garny, E. Tsati, and K. Dahlmann, *Aircraft routing with minimal climate impact: the REACT4C climate cost function modelling approach (V1. 0).* Geoscientific Model Development, 2014. 7: p. 175-201.
8. Matthes, S., U. Schumann, V. Grewe, C. Frömming, K. Dahlmann, A. Koch, and H. Mannstein, *Climate Optimized Air Transport*, in *Atmospheric Physics: Background – Methods – Trends*, U. Schumann, Editor. 2012, Springer Berlin Heidelberg: Berlin, Heidelberg. p. 727-746.
9. Frömming, C., V. Grewe, S. Brinkop, A.S. Haselrud, S. Matthes, E.A. Irvine, S. Rosanka, and J. van Manen, *Infuence of weather situation on aviation emission effects: The REACT4C Climate Change Functions.* in preparation for Atmos. Environm., 2017.
10. Grewe, V., S. Matthes, C. Frömming, S. Brinkop, P. Jöckel, K. Gierens, T. Champougny, J. Fuglestvedt, A. Haslerud, E. Irvine, and K. Shine, *Feasibility of climate-optimized air traffic routing for trans-Atlantic flights.* Environmental Research Letters, 2017. 12(3).
11. Verbist, P., *Green Flight Trajectories-A REACT4C data analysis*. 2016, Delft University of Technology: Delft.
12. Irvine, E.A., B.J. Hoskins, K.P. Shine, R.W. Lunnon, and C. Froemming, *Characterizing North Atlantic weather patterns for climate-optimal aircraft routing.* Meteorological Applications, 2013. 20(1): p. 80-93.
13. Jöckel, P., A. Kerkweg, A. Pozzer, R. Sander, H. Tost, H. Riede, A. Baumgaertner, S. Gromov, and B. Kern, *Development cycle 2 of the Modular Earth Submodel System (MESSy2).* Geosci. Model Dev., 2010. 3(2): p. 717-752.
14. Jöckel, P., R. Sander, A. Kerkweg, H. Tost, and J. Lelieveld, *Technical Note: The Modular Earth Submodel System (MESSy) - a new approach towards Earth System Modeling.* Atmos. Chem. Phys., 2005. 5(2): p. 433-444.
15. Jöckel, P., H. Tost, A. Pozzer, M. Kunze, O. Kirner, C.A.M. Brenninkmeijer, S. Brinkop, D.S. Cai, C. Dyroff, J. Eckstein, F. Frank, H. Garny, K.-D. Gottschaldt, P. Graf, V. Grewe, A. Kerkweg, B. Kern, S. Matthes, M. Mertens, S. Meul, M. Neumaier, M. Nützel, S. Oberländer-Hayn, R. Ruhnke, T. Runde, R. Sander, D. Scharffe, and A. Zahn, *Earth System Chemistry integrated Modelling (ESCiMo) with the Modular Earth Submodel System*

(MESSy) version 2.51. Geosci. Model Dev., 2016. 9(3).

16. Roeckner, E., R. Brokopf, M. Esch, M. Giorgetta, S. Hagemann, L. Kornblueh, E. Manzini, U. Schlese, and U. Schulzweida, *Sensitivity of simulated climate to horizontal and vertical resolution in the ECHAM5 atmosphere model.* Journal of Climate, 2006. 19(16): p. 3771-3791.
17. Roeckner, E., G. Bäuml, L. Bonaventura, R. Brokopf, M. Esch, M. Giorgetta, S. Hagemann, I. Kirchner, L. Kornblueh, and E. Manzini, *The atmospheric general circulation model ECHAM 5. PART I: Model description*, E. Roeckner, et al., Editors. 2003, Max Planck Institute for Meteorology: Hamburg.
18. Yamashita, H., V. Grewe, P. Jöckel, F. Linke, M. Schaefer, and D. Sasaki, *Air traffic simulation in chemistry-climate model EMAC 2.41: AirTraf 1.0.* Geosci. Model Dev., 2016. 9(9): p. 3363-3392.
19. Grewe, V., E. Tsati, M. Mertens, C. Frömming, and P. Jöckel, *Contribution of emissions to concentrations: The TAGGING 1.0 submodel based on the Modular Earth Submodel System (MESSy 2.52).* Geosci. Model Dev. Discuss., 2017. 2017: p. 1-33.
20. Dietmüller, S., P. Jöckel, H. Tost, M. Kunze, C. Gellhorn, S. Brinkop, C. Frömming, M. Ponater, B. Steil, A. Lauer, and J. Hendricks, *A new radiation infrastructure for the Modular Earth Submodel System (MESSy, based on version 2.51).* Geosci. Model Dev., 2016. 9(6): p. 2209-2222.
21. Yamashita, H., V. Grewe, P. Jöckel, F. Linke, M. Schaefer, and D. Sasaki. *Towards Climate Optimized Flight Trajectories in a Climate Model: AirTraf*. in *USA/Europe Air Traffic Management Research and Development Seminar*. 2015.
22. Eurocontrol, *User Manual for the Base of Aircraft Data(BADA) Revision 3.9*, in *EEC Technical/Scitific Report*. 2011.
23. Deidewig, F., A. Döpelheuer, and M. Lecht, *Methods to assess aircraft engine emissions in flight*, in *20th Congress of the International Council of the Aeronautical Sciences* 1996: Sorrento, Italy. p. 131-141.
24. *ICAO technical report-ICAO Engine Exhuast Emission Data*. 2005: ICAO: Montreal, QC, Canada.
25. Grewe, V. and A. Stenke, *AirClim: an efficient tool for climate evaluation of aircraft technology.* Atmos. Chem. Phys., 2008. 8(16): p. 4621-4639.
26. Sasaki, D., S. Obayashi, and K. Nakahashi, *Navier-Stokes optimization of supersonic wings with four objectives using evolutionary algorithm.* Journal of Aircraft, 2002. 39(4): p. 621-629.
27. Sasaki, D. and S. Obayashi, *Efficient Search for Trade-Offs by Adaptive Range Multi-Objective Genetic Algorithms.* Journal of Aerospace Computing, Information, and Communication, 2005. 2(1): p. 44-64.
28. Søvde, O.A., S. Matthes, A. Skowron, D. Iachetti, L. Lim, B. Owen, Ø. Hodnebrog, G. Di Genova, G. Pitari, D.S. Lee, G. Myhre, and I.S.A. Isaksen, *Aircraft emission mitigation by changing route altitude: A multi-model estimate of aircraft NOx emission impact on O3 photochemistry.* Atmospheric Environment, 2014. 95(0): p. 468-479.